U-Co Bimetallic-Organic Framework Showing Helical 1D Pore Decorated by Abundant -CH_3 Groups: Robust Nature under Acid, Base, and Water for High-Performance SO_2 Removal

Ying Xu, Yaling Fan, Xue Feng Feng, and Feng Luo*

School of Chemistry, Biology and Materials Science, East China University of Technology, Nanchang 330013, China, E-mail: ecitluofeng@163.com

Experimental Methods

Materials and Physical Measurements. All chemicals are directly purchased from innochem with no further purification. The data of X-ray powder diffraction were collected on a Bruker AXSD8 Discover powder diffractometer at 40 kV/40 mA for Cu Kα (λ = 1.5406 Å) at room temperature in the range of 5-50 °(2θ) with a scan speed of 0.1 °per step. Thermogravimetric analysis (TG) was performed by a TGA Q500 thermal analysis system. All TGA experiments were performed under a N_2 atmosphere from 40-800°C at a rate of 5°C /min. The gas sorption isotherms were collected on ASAP2020 PLUS (anti-corrosion version). Ultrahigh-purity-grade (>99.999%) N_2, CO_2, and SO_2 gases were used in this adsorption measurement. To maintain the experimental temperatures liquid nitrogen (77 K) and temperature-programmed water bath (273 and 298 K) were used respectively.

Synthesis of ECUT-123. $Co(NO_3)_2 \cdot 6H_2O$ (0.1 mmol, 29.1 mg), uranyl nitrate (0.1 mmol, 50 mg) and 2-methyl-2H-imidazole-4,5-dicarboxylic acid (0.1 mmol, 19 mg) were dissolved in a mixture of 1 mL H_2O and 4 mL N,N′-dimethylformamide in the presence of concentrated nitric acid (0.1 mL). The solution was moved into a 25 mL Teflon-lined stainless steel vessel and heated at 120 °C for 3 days. Then it is cooled down to room temperature. Pink crystals were filtered and washed with 10 mL ethanol and 10 mL deionized water. The yield was 81% based on Co(II). Element analysis (%): calc. C/24.88, N/10.27, H/2.67; exp. C/24.56, N/10.19, H/2.74.

Degassing ECUT-123. 100 mg MOF crystals were soaked in methanol for 3d and fresh methanol was added every 8 h. After decanting the methanol extract, the sample was dried at room temperature overnight, then further degassed using ASAP2020 PLUS for 24 h at 150°C.

Chemical and water stability test. 100 MOF crystals were soaked in corresponding solution such as water or pH=2 or pH=12 solution for one week. Then, the resulted samples were characterized by PXRD and N_2 adsorption. Note that before N_2 adsorption, the activation process should be carried out.

X-ray Crystallography. X-ray diffraction data of ECUT-123 was collected at room temperature on a Bruker Appex II CCD diffractometer using graphite monochromated MoKα radiation (λ=0.71073 Å). The data reduction included a correction for Lorentz and polarization effects, with an applied multi-scan absorption correction (SADABS). The crystal structure was solved and refined using the SHELXTL program suite. Direct methods yielded all non-hydrogen atoms, which were refined with anisotropic thermal parameters. All hydrogen atom positions were calculated geometrically and were riding on their respective atoms. The SQUEEZE subroutine of the PLATON software suite was used to remove the scattering from the highly disordered guest molecules. CCDC 2103848 contains the supplementary crystallographic data of ECUT-123. These data can be obtained free of charge from the Cambridge Crystallographic Data Centre via

www.ccdc.cam.ac.uk/data_request/cif.

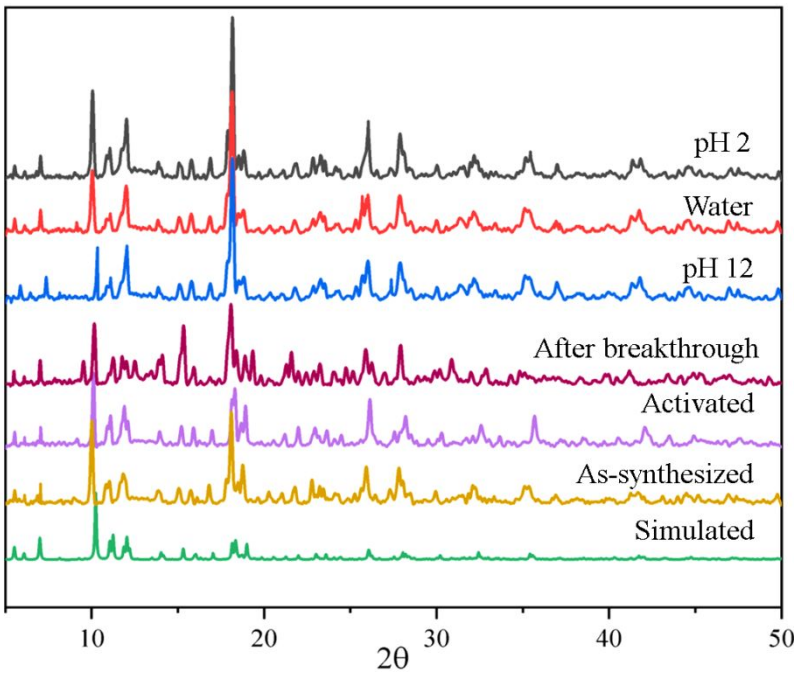

Figure S1. A comparison of PXRD results among the simulated data from single crystal data, as-synthesized samples, and the samples under different conditions.

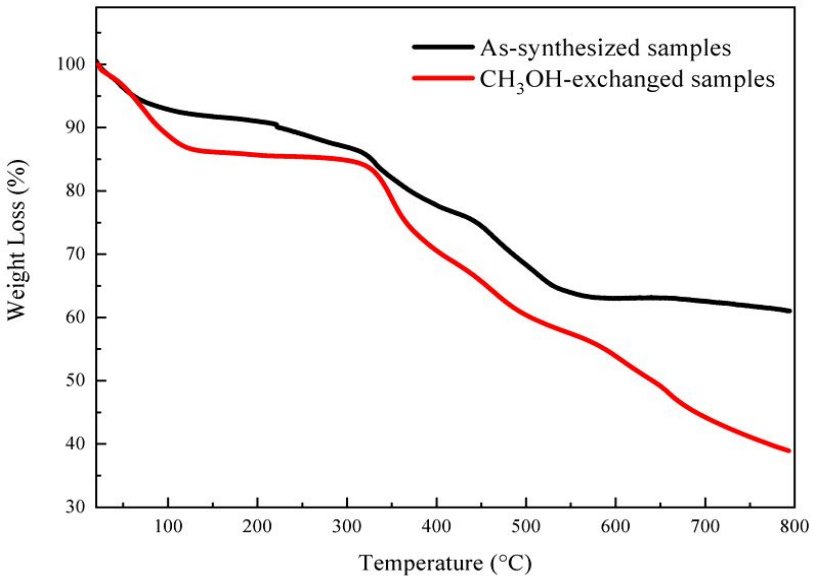

Figure S2. The TG plots of the as-synthesized samples and the CH3OH-exchanged samples.

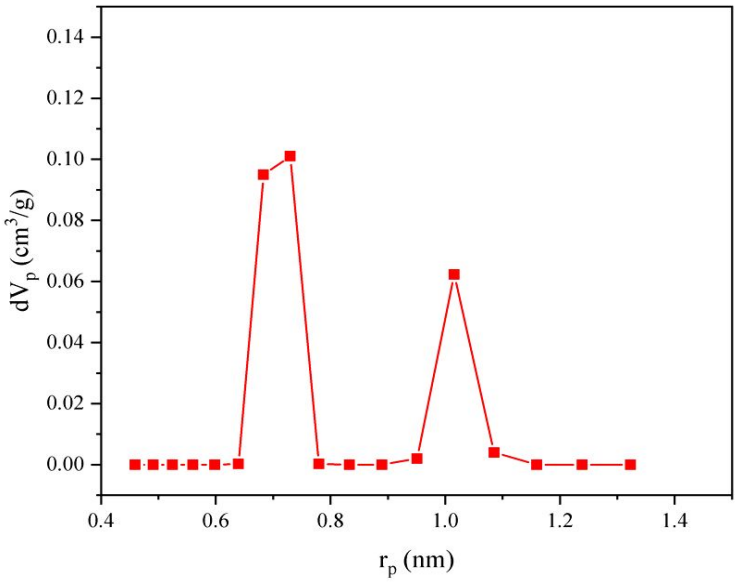

Figure S3. The pore size distribution of ECUT-123.

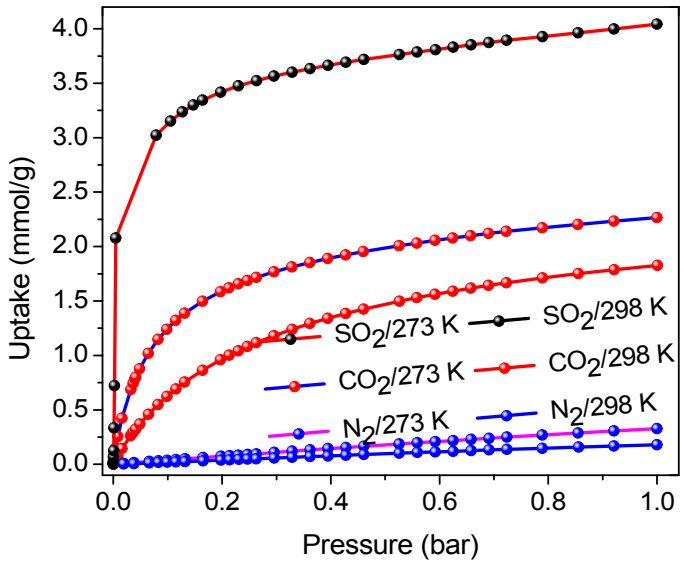

Figure S4. The SO_2, CO_2, and N_2 adsorption isotherms at 298 K and 273 K.

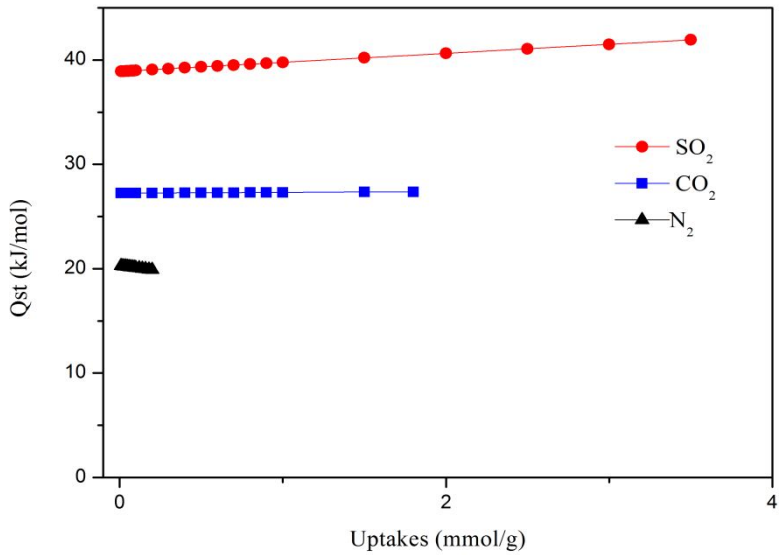

Figure S5. The calculated adsorption heat enthalpy of SO_2, CO_2 and N_2.

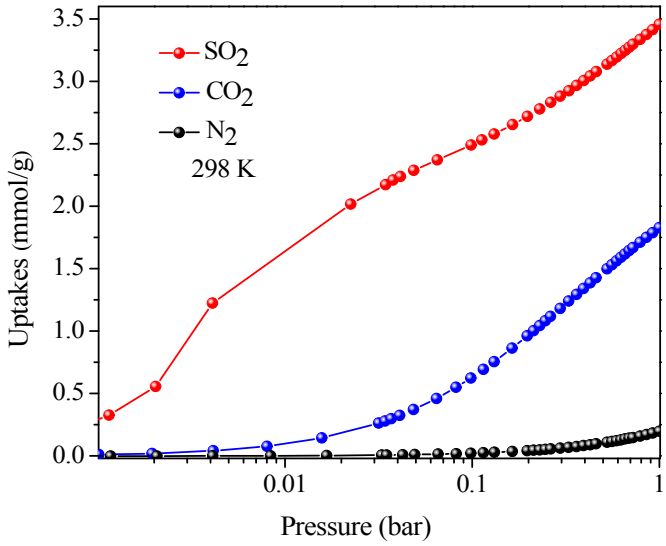

Figure S6. The SO_2, CO_2, and N_2 adsorption isotherm at low pressure.

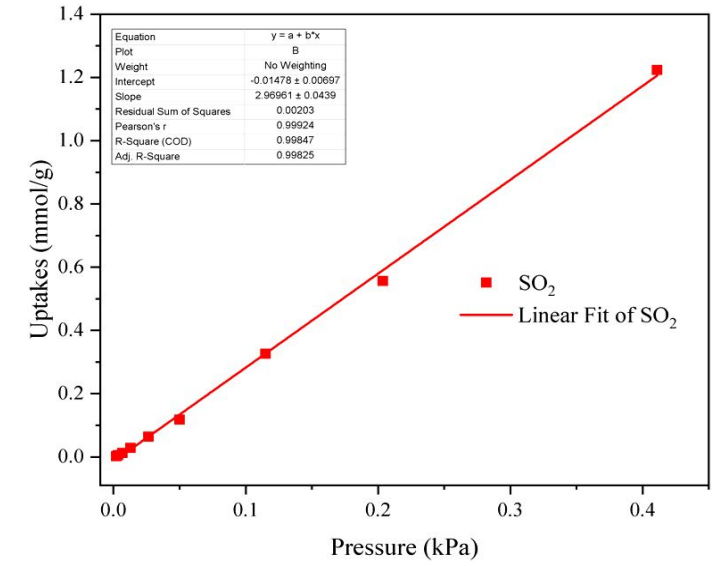
Equation y = a + b*x
Plot B
Weight No Weighting
Intercept -0.01478 ± 0.00697
Slope 2.96961 ± 0.0439
Residual Sum of Squares 0.00203
Pearson's r 0.99924
R-Square (COD) 0.99847
Adj. R-Square 0.99825
Uptakes (mmol/g)
Pressure (kPa)
SO2
Linear Fit of SO2

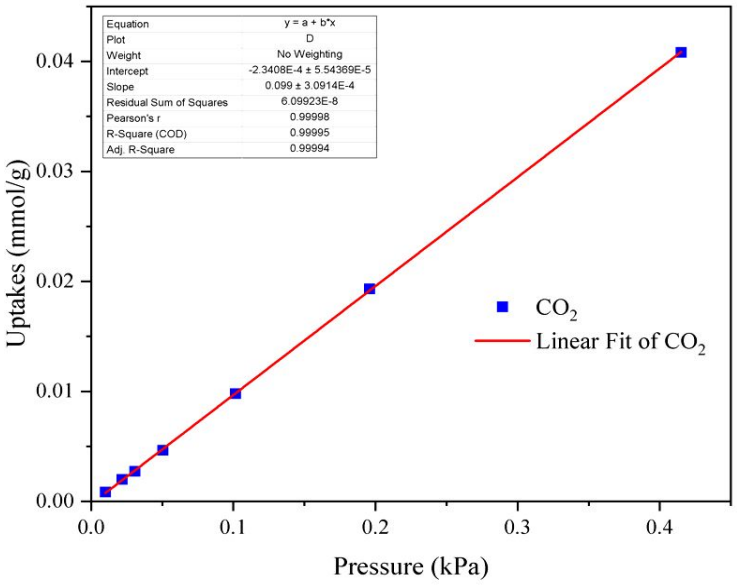
Equation y = a + b*x
Plot D
Weight No Weighting
Intercept -2.3408E-4 ± 5.54369E-5
Slope 0.099 ± 3.0914E-4
Residual Sum of Squares 6.09923E-8
Pearson's r 0.99998
R-Square (COD) 0.99995
Adj. R-Square 0.99994
Uptakes (mmol/g)
Pressure (kPa)
CO2
Linear Fit of CO2

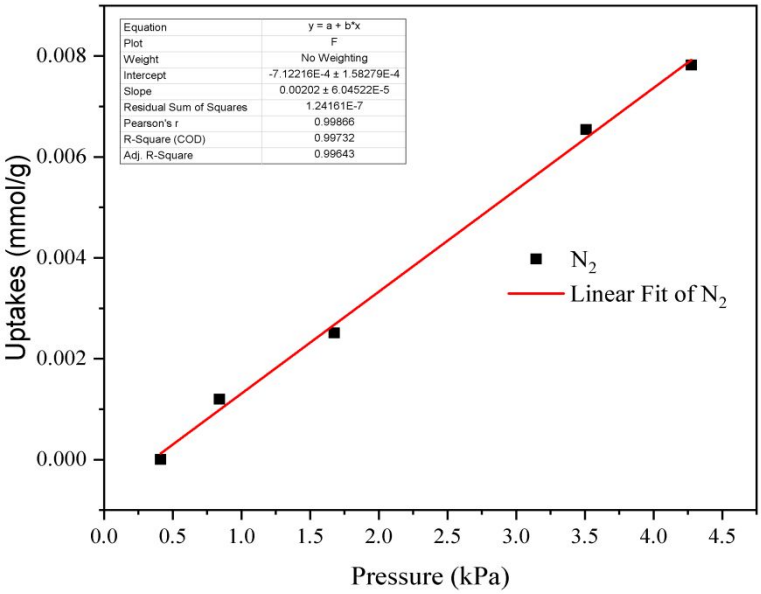
Equation y = a + b*x
Plot F
Weight No Weighting
Intercept -7.12216E-4 ± 1.58279E-4
Slope 0.00202 ± 6.04522E-5
Residual Sum of Squares 1.24161E-7
Pearson's r 0.99866
R-Square (COD) 0.99732
Adj. R-Square 0.99643
Uptakes (mmol/g)
Pressure (kPa)
N2
Linear Fit of N2

Figure S7. The calculation of Henry's constant.

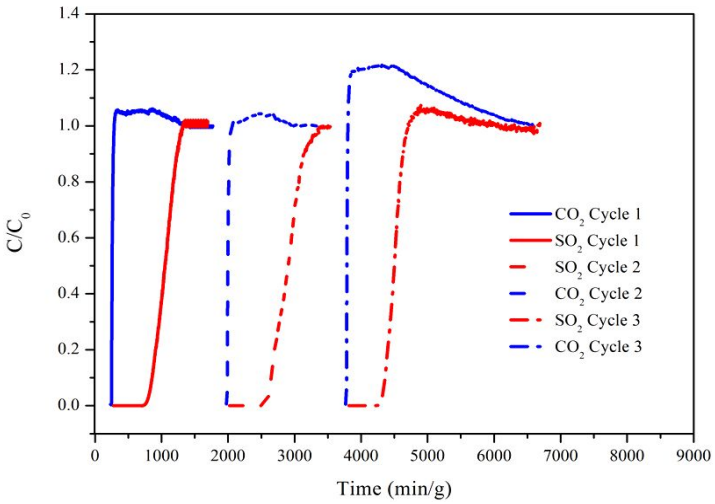

Figure S8. The repeating breakthrough tests for ECUT-123.

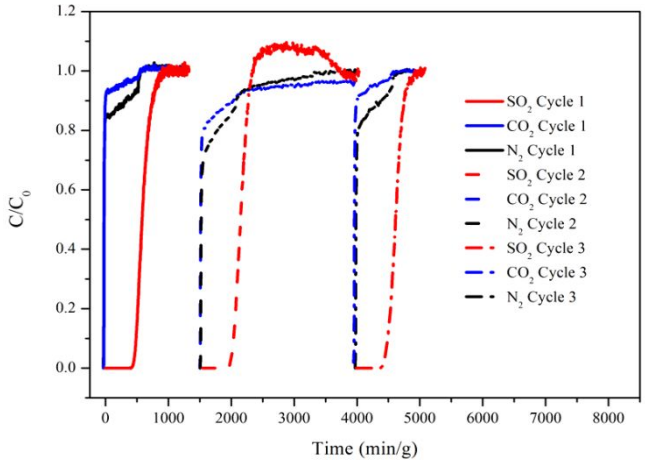

Figure S9. The repeating breakthrough tests for ECUT-123.

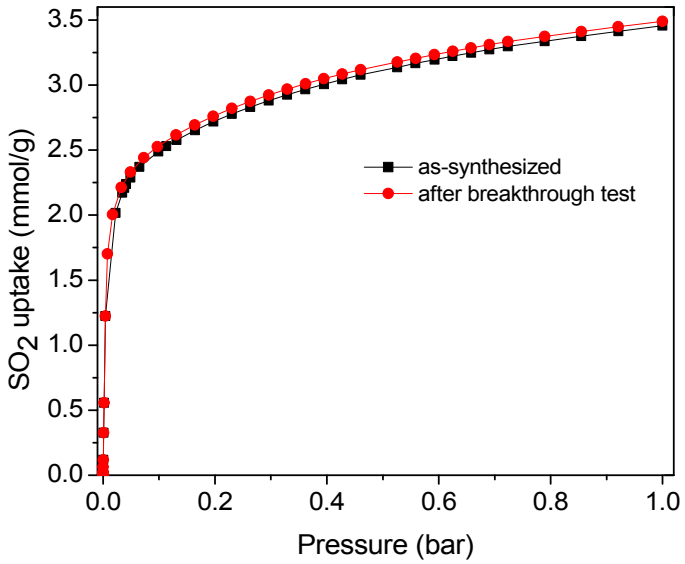

Figure S10. A comparison of the SO_2 adsorption for the as-synthesized samples and samples after all breakthrough tests.

Table S1. A crystallographic summary of ECUT-123.

Compound	ECUT-123
Crystal system	Tetragonal
Space group	$P4_32_12$
Unit cell dimensions	a=20.5147(7) Å b=20.5147(7) Å c=25.5520(17) Å
Volume	10753.6(9) Å ^{3}
Z, Calculated density	8, 1.685 mg/m^3
F(000)	5020
Completeness to theta = 25.00	99.9 %
R indices (all data)	R1=0.0954, wR2=0.2358
Absolute structure parameter	0.2(3)
CCDC number	2103848

Table S2. A comparison of SO_2 adsorption between reported materials and ECUT-123.

MOF tpyes	SO_2 adsorption capacity (1 bar, 298 K), mmol/g	SO_2/CO_2 selectivity	References
SIFSIX-2-Cu-i	11.0	87.1	1
$Ni(bdc)(ted)_{0.5}$	9.97	-	2
MFM-300(In)	8.28	50	3
MFM-202a	10.2	-	4
NOTT-300 (Al)	7.1	-	5
MFM-170	17.5	28	6
MOF-5	Less than 0.016	-	7
IRMOF-3	0.094	-	7
MOF-74	3.03	-	7
MOF-199	0.5	-	7
P(TMGA-co-MBA)	4.0	-	8
Activated Carbon	3.3	-	9
Cage-U-Co-MOF	3.62	80.7	10
ECUT-111	11.56	25.2	11
ECUT-100	4.95	26.9	12
ECUT-123	3.45	32.1	This work

"-" denotes the data cannot be obtained from corresponding reference.

1.Cui. X. L.; Yang. Q. W.; Yang. L. F.; Krishna. R.; Zhang. Z. G.; Bao. Z. B.; Wu. H.; Ren. Q.; Zhou. W.; Chen. B. L.; Xing. H. B. Ultrahigh and selective SO_2 uptake in inorganic anion-pillared hybrid porous materials. *Advanced Materials*. **2017**. *29*.1606929(1-9).

2. Tan. K.; Canepa. P.; Gong. Q. H.; Liu. J.; Johnson. D. H.; Dyevoich. A.; Thallapally. P. K.; Thonhauser. T.; Li. J.; Chabal. Y. J. Mechanism of preferential adsorption of SO_2 into two microporous paddle wheel frameworks $M(bdc)(ted)_{(0.5)}$. *Chemistry of Materials*. **2013**. *25*.

4653-4662.

3. Savage. M.; Cheng .Y. Q.; Easun. T. L.; Eyley. J. E.; Argent.S. P.; Warren. M. R.; Lewis. W.; Murray. C.; Tang. C. C.; Frogley. M. D.; Cinque G.; Sun. J. L.; Rudic´. S.; Murden R. T.; Benham. M. J.; Fitch. A. N.; Blake. A. J.; Ramirez-Cuesta. A. J.; Yang. S. H.; Schroder. M. Selective Adsorption of Sulfur Dioxide in a Robust Metal–Organic Framework Material. *Advanced Materials*. **2016**. *28*. 8705-8711.

4. Yang. S. H.; Liu. L. F.; Sun. J. L.; Thomas. K. M.; Davies A. J.; George. M. W.; Blake. A. J.; Hill. A. H.; Fitch. A. N.; Tang. C. C. , Chroeder. M. Irreversible network transformation in a dynamic porous host catalyzed by sulfur dioxide. *Journal of the American Chemical Society*. **2013**. *135*. 4954-4957.

5. Yang. S. H.; Sun. J. L.; Ramirez-Cuesta. A. J.; Callear. S. K.; David. W. F.; Anderson. D. P.; Newby. R.; Blake. A. J.; Parker. J. E.; Tang. C. C.; Schro¨der1. M. Selectivity and direct visualization of carbon dioxide and sulfur dioxide in a decorated porous host. *Nature chemistry.* **2012**. *4*.887-894.

6. Smith. G. L.; Eyley. J. E.; Han. X.; Zhang. X. R.; Li. J. N.; Jacques. N. M.; Godfrey. H. G. W.; Argent. S. P.; McPherson. L. J. M.; Teat. S. J.; Cheng Y. Q.; Frogley. M. D.; Cinque. G.; Day S. J.; C. C. Tang.; Easun . T. L.; Rudić. S.; Ramirez-Cuesta . A. J.; Yang. S.H.; Schro¨der1. M. Reversible coordinative binding and separation of sulfur dioxide in a robust metal–organic framework with open copper sites. *Nature Materials.* **2019**. *18*. 1358-1365.

7. Britt. D.; Tranchemontagne. D.; Yaghi O. M. Metal-organic frameworks with high capacity and selectivity for harmful gases. *Proceedings of the National Academy of Sciences of the United States of America*. **2008**. *105*. 11623-11627.

8. Wu. L. B.; An. D.; Dong. J.; Zhang. Z. M.; Li. B. G.; Zhu. S. P. Preparation and SO2 Absorption/Desorption Properties of Crosslinked Poly(1,1,3,3-Tetramethylguanidine Acrylate) Porous Particles. *Macromolecular Rapid Communications*. **2006**. *37*.1949-1954.

9. Yi. H. H.; Wang. Z. X.; Liu. H.Y.; Tang X. L.; Ma. D.; Zhao. S. Z.; Zhang. B. W.; Gao. F. Y.; Zuo Y. R. Adsorption of SO_2, NO, and CO_2 on Activated Carbons: Equilibrium and Thermodynamics . *Journal of Chemical & Engineering Data.* **2014**. *59*. 1556-1563.

10. Fan, Y. L.; Yin, M. J.; Krishna, R.; Feng, X. F.; Luo, F. Constructing a robust gigantic drum-like hydrophobic [$Co_{24}U_6$] nanocage in a metal–organic framework for high-performance SO_2 removal in humid conditions. *J. Mater. Chem. A* **2021**, *9*, 4075–4081.

11. Yin, M. J.; Xiong, X. H.; Feng, X. F.; Xu, W. Y.; Krishna, R.; Luo, F. A Robust Cage-Based Metal−Organic Framework Showing Ultrahigh SO_2 Uptake for Efficient Removal of Trace SO_2 from

SO_2/CO_2 and $SO_2/CO_2/N_2$ Mixtures. *Inorg. Chem.* **2021**, *60*, 3447−3451.

12. Guo, L. J.; Feng, X. F.; Gao, Z.; Krishna, R.; Luo, F. Robust 4d−5f Bimetal−Organic Framework for Efficient Removal of Trace SO_2 from SO_2/CO_2 and $SO_2/CO_2/N_2$ Mixtures. *Inorg. Chem.* **2021**, *60*, 1310−1314.